Journal of Systems Engineering and Electronics
Vol. 37, No. 3, June 2026, pp.974 – 992

An evaluation framework for equipment contribution rate to system of systems based on operation loop and improved Shapley value

HU Cancan and WANG Yaping*

School of Mechanical Engineering, Nanjing University of Science and Technology, Nanjing 210094, China

Abstract: The evaluation of the equipment contribution rate to system-of-systems (CRSoS) is crucial for optimizing the armament system-of-systems structure and enhancing combat effectiveness. The traditional relative contribution rate method poses limitations by focusing on individual equipment evaluation without considering the interrelations between equipment. In response to the issue, this study proposes a framework based on operation loop and improved Shapley value (OLISV) for analysis to ananlyze the equipment CRSoS. Specifically, a multi-layer network model is first constructed based on complex heterogeneous network and operation loop theory. Next, information entropy and evidence theory are used for the edges of the functional node layer, while improving the parallel node structure within the network. Subsequently, an improved Shapley value contribution rate method based on non-efficiency influencing factors is proposed. Finally, the rationality and effectiveness of the OLISV are illustrated through a case study.

Keywords: operation loop, heterogeneous networks, armament system-of-systems, contribution rate, improvement of Shapley value.

DOI: 10.23919/JSEE.2026.000117

1. Introduction

With the rapid development of information technology over the past three decades in the military, army operating concepts such as network-centric warfare, mosaic warfare, hybrid warfare, etc., are proposed and applied. The functions of military forces have grown increasingly complex and diversified, prompting a gradual shift in operational patterns from platform-centric warfare to system confrontation [1]. The armament system-of-systems (ASoS) is composed of various types of military equipment, within its overall effectiveness is reliant on the interrelated and cooperative functions among them [2,3]. Recently, equipment-oriented analysis of contribution rate to system-of-systems (CRSoS) has been a growing emphasis. The accurate and effective measurement of each equipment's contribution within the ASoS is integral for demonstrating and developing the ASoS as well as for structural optimization.

Currently, the definition of CRSoS focuses on its role in contributing to fulfilling operational tasks, meeting operational capability requirements, adapting to system function, and optimizing system structure. The concept of CRSoS is primarily composed of three main aspects, CRSoS of structure, CRSoS of mission effectiveness, and CRSoS of performance [4].

The CRSoS of structure assesses the impact of the presence or absence of the equipment on the system performance enhancement, which includes the overall structural performance and the system network structure [5,6] and other aspects. The CRSoS of mission effectiveness assesses the impact of the presence or absence of equipment on the fulfillment of the operational tasks, which includes the operational mission [7,8], the mission chain [9] and so on. The CRSoS of performance assesses the impact of equipment on the system's capability or effectiveness. Therein system capability assesses the equipment on their combat capability enhancement or the enemy combat capability decline in the degree of contribution [10,11], and system effectiveness assesses the use of a piece of equipment before and after the degree of enhancement of the combat effectiveness [12].

Due to the different concepts of CRSoS, the focus of the assessment methods varies depending on assessment objectives, including mathematical analysis, exploratory analysis, operation simulation, uncertainty reasoning, operation loops, complex networks, and deep learning [13–15]. Among them, the operation loop-based assess-

Manuscript received May 31, 2024.
*Corresponding author.
This work was supported by the National Defense Basic Scientific Research Program of China (JCKY2021209B017).

ment method classifies and describes the functional nodes and edges in the ASoS while considering the correlation relationships between the equipment. This method incorporates the observation-oriention-decision-action (OODA) theory, which enables a more realistic portrayal of the operational process and has been validated as an effective approach for analyzing CRSoS.

Many scholars have carried out research work based on operation loops. Tan et al. [16] took the lead in proposing an equipment architecture modeling method based on an operation loop, analyzed the impact of system topology on system capability, and gave comprehensive evaluation indexes of the operation loop as well as example validation. Pan et al. [17] conducted a resilience-based importance measure analysis to optimization the structure of the SoS. Yang et al. [18] proposed, for the first time, a multi-objective optimization algorithm called the multi-objective ant colony evolutionary algorithm based on decomposition (MOACEA/D). They pioneered the operation loop recommendation problem by using operation ring quality as the optimization objective and closed-loop time as the constraint. Furthermore, they established a corresponding planning model, thereby achieving operation loop recommendation. Zhou et al. [5] introduced integrated equipment into the operation loop for modeling, and combined it with the reliability of the network to give the disjointed minimal path and the Monte Carlo based on the spectral radius, and proposed the CRSoS model after the introduction of integrated equipment. Luo et al. [19] argued that, considering the heterogeneity of various equipment and their associated relationships, the combat effectiveness of the equipment system increases with the number of combat rings, and then proposed a CRSoS evaluation method based on operation loop and information entropy. Shao et al. [20] developed an equivalent transfer function algorithm based on characteristic functions and transfer probabilities, utilizing the graphical evaluation and review technique (GERT). Through an in-depth analysis of communication link importance metrics, they derived algorithmic formulations for both communication link effectiveness and importance assessment. Based on these findings, they established the PS-G-GERT effectiveness evaluation model, specifically designed for assessing geostationary Earth orbit (GEO) satellite communication constellation effectiveness under conditions of information deficiency. Wang et al. [21] proposed an equivalent transfer function applicable to the SoS-GERT network based on the moments' mother function and Mason's formula, gave a formula for the system combat effectiveness, and constructed a CRSoS assessment model. Han et al. [3] constructed a regional air defense anti-missile system network model and proposed an assessment method based on the number of operation loops and the amount of self-information, as well as analyzing and studying the network resilience metric under different attack and recovery strategies.

However, there are some problems in the above research. First, the object of CRSoS analysis is single equipment, and it is not decomposed to the level of functional nodes. Additionally, for the structure of parallel nodes in the combat network, the calculation fails to consider the weight relationship between the nodes. The research predominantly relies on the relative contribution rate (RCR) model for computation, which attributes the change in combat effectiveness solely to the presence or absence of equipment, disregarding the characteristics of the system itself, such as coupling and emergence [22]. Moreover, when analyzing the parallel node structure in the combat network, the weight relationship between nodes is not taken into account in the calculation.

In light of these issues, this paper introduces the Shapley value and considers the evaluation of CRSoS as a cooperative game. The Shapley value distributes the returns based on the marginal contribution among the participating members of the coalition and is considered to be an equitable distribution principle that achieves an efficient equilibrium subject to the condition of additivity [23]. The Shapley value has found application in a diverse array of fields such as resource sharing and benefit allocation [24,25], coordinated optimization of energy systems electricity cost sharing [26,27], water allocation [28], machine learning [29,30] and benefit subsidies [31]. Tao et al. [32] constructed a gray ADC effectiveness assessment model and proposed a CRSoS assessment method based on the gray Shapley value. Li et al. [33] developed a two-layer road data asset revenue allocation model based on a modified Shapley value approach. This comprehensive model incorporates three key components: (i) a revenue allocation evaluation index system, (ii) a hybrid weighting methodology combining entropy weighting with rough set theory, and (iii) utilizing fuzzy comprehensive evaluation and numerical analysis to quantify participant contribution levels. Fang et al. [25] established a cooperative game scheduling model of combined heat and power-virtual power plant and proposed an improved Shapely value method to achieve optimal benefit allocation. Le et al. [34] proposed a stochastic algorithm combining linear programming sensitivity analysis and stratified sampling technique to solve the Shapley value of the large-scale linear production game. Wang et al. [35] introduced an innovative variation coefficient-Shapley value method for compensation benefit allocation in multi-owner cascade hydropower systems. This methodology integrates individual characteristic weight coefficients with the Shapley value for each hydropower station, demonstrating its effectiveness in achieving equitable and rational compensation benefit distribution among cascade hydropower stations. However, the above studies did not take into account the issue of redistributing the contribution of the same type of participating members in the member alliance, i.e., the same type of equipment.

To address the deficiencies described above, this paper constructs a three-layer network model of task-equipment-function, utilizing the theory of mission decomposition and operation loop. The object of CRSoS analysis is extended to the functional layer of equipment and improves the calculation method of the parallel structure of the functional nodes. After that, the CRSoS calculation method based on the improved Shapley value method is proposed.

2. Modeling of ASoS networks

2.1 Theoretical basis of operation loop

The concept of the operation loop (Fig. 1) is derived from the OODA theory, which represents a high level of abstraction of the combat process [36]. This modeling idea aims to analyze the flow of information in combat by incorporating the enemy target into the modeling process and categorizes combat entities based on their roles in the weapon and equipment system into Sensor (S), Decision (D), Influence (I) and Target (T) [16]. The basic process of the operation loop involves the reconnaissance unit discovering the enemy target and transmitting the target information to the decision unit. The decision unit then analyzes the intelligence, posture, and other information to issue an attack command to the influence unit. Subsequently, the influence unit receives the command and executes an attack on the enemy target. Within this cycle, numerous operation loops are formed, with each loop encompassing different operational entities within the ASoS.

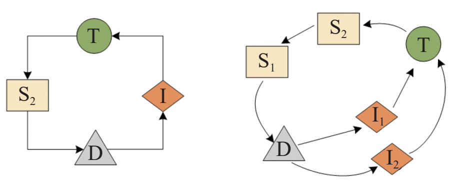

Fig. 1 Operation loop

2.2 Heterogeneous network modeling

Due to the existence of equipment with multiple operational functions in the ASoS at the squad level, such as unmanned aerial vehicles (UAVs) at the same time with reconnaissance, strike, and other functions. In different operational task stages, the equipment assumes different roles, and the information interaction between the equipment is close. Reasonably extracting the relationships between equipment entities and their functions within the equipment system and constructing a network model that aligns with actual combat scenarios are essential prerequisites for effective assessment and analysis [37]. In this paper, the multi-layer network (Fig. 2) method is utilized to construct the combat network model of the ASoS, which comprises the operational task layer, equipment layer, and functional node layer. The operational task layer represents the specific combat task derived from mission decomposition, the equipment layer denotes the equipment entity within the ASoS, and the functional node layer signifies the corresponding combat function of the equipment entity.

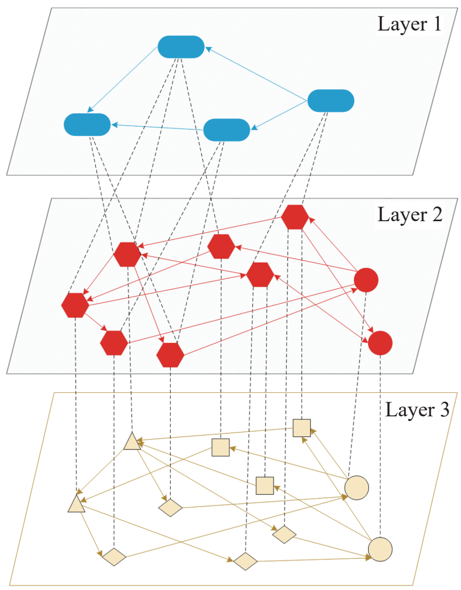

Fig. 2 Multi-layer heterogeneous network

The operational task layer decomposes the operational mission into specific sub-tasks through task decomposition, and the sub-tasks at different stages correspond to different equipment allocation schemes.The equipment allocation plan for reconnaissance missions focuses on selecting reconnaissance equipment, while the equipment allocation plan for strike missions primarily revolves around configuring firepower-strike equipment. The equipment entities in the equipment layer are obtained through the task layer.

The equipment layer (Fig. 3) represents the equipment entities, where equipment with single function (ESF) is considered a single type of equipment, and equipment with multiple functions (EMF) is regarded as a comprehensive type of equipment, and equipment is classified according to different system types. Due to the multifunctional nature of integrated equipment, the equipment layer forms a bidirectional interaction relationship, which can complicate analysis and calculation and obtain the functional node layer by reasonably extracting the relationships between equipment entities and their functions within the equipment system.

The functional node layer signifies the corresponding combat function of the equipment entity, with the coupling relationship between the equipment layer and functional node layer including both "one-to-one" and "one-to-many" relationships. Establish a unidirectional combat loop at the functional node layer. Model the functional node layer to obtain combat effectiveness and calculate the CRSoS of the functional nodes. Then, use the weighted aggregation method to obtain the system contribution rate of the equipment. Specifically: firstly, a CRSoS assessment of functional nodes within the functional layer for a single mission is conducted, then the results upward is aggregated to determine the CRSoS of the equipment, and finally the CRSoS of the equipment is derived for the entire mission phase.

The functional node layer network is a directed network consisting of an exhaustive non-empty node set N and a set of connected edges L [38], which can be described by the following equations:

$$G = (N,L),$$

$$N = N_{\mathrm{T}} \cup N_{\mathrm{s}} \cup N_{\mathrm{D}} \cup N_{\mathrm{I}} = (n_1, n_2, \cdots, n_k),$$

$$L = l_{ij},$$

where N denotes the set of equipment function nodes, consisting of target class nodes, sensor class nodes, decision class nodes, and influence class nodes; $L = l_{ij}$ is the set of connecting edges between function nodes in the combat network.

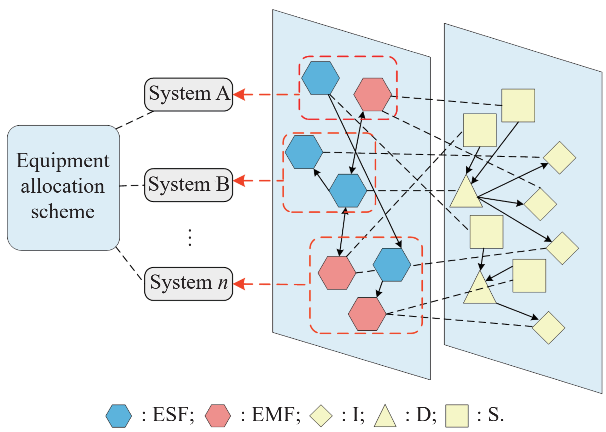

Fig. 3 Modelling of the equipment layers

2.2.1 Modeling of nodes

Based on the categorization of the four types of weapon and equipment nodes (S, D, I, and T) within the operation loop, modeling is conducted for each type of node in the ASoS. By considering the information transfer roles between these nodes, a generalized communication capability term is established, and capability calculation index terms are provided for each type of node. Let the equipment system functional node capability set be C_i, which can be expressed as

$$C_i = \{C_{\mathrm{S}}, C_{\mathrm{D}}, C_{\mathrm{I}}, C_{\mathrm{T}}, C_{\mathrm{C}}\}$$

where C_{S} denotes sensor-type functional node; C_{D} denotes decision-type functional node; C_{I} denotes influence-type functional node; C_{T} denotes target-type node; C_{C} denotes communication functional item.

Further, the functional node capability indicator term can be represented as

$$c_i^j = \left\{c_{\mathrm{S}}^1, c_{\mathrm{S}}^2, \cdots, c_{\mathrm{S}}^m\right\}$$

where m denotes the number of functional node capacity indicator items.

As shown in Table 1, the capability indicators considered for S nodes are maneuvering speed, maximum detecting distance, detecting accuracy, identifying probability, and tracking probability; the capability indicators considered for D nodes are decision-making time, decision-making accuracy, and assisted decision-making; the capability indicators considered for I nodes are maneuvering speed, damaging radius, striking accuracy, and effective range; the capability indicators that need to be considered for the T category are maneuvering speed, warning time, destructive capability, and stealth capability; the capability indicators that need to be considered for communication capability are communication coverage, communication rate, communication capacity, communication delay, and communication quality [39].

Table 1 Capability indicator decomposition

Entity	Capability symbol	Indicator	Indicator symbol	Unit	Type
S	C_{S}	Maneuvering speed	c_{S}^1	km/h	Benefit
		Maximum detecting distance	c_{S}^2	km	Benefit
		Detecting accuracy	c_{S}^3	m^2	Benefit
		Identifying probability	c_{S}^4	0 – 1	Benefit
		Tracking probability	c_{S}^5	0 – 1	Benefit

Continued

Entity	Capability symbol	Indicator	Indicator symbol	Unit	Type
D	$C_{\rm D}$	Decision making time	$c_{\rm D}^1$	s	Cost
		Decision-making accuracy	$c_{\rm D}^2$	0 – 1	Benefit
		Assisted decision making	$c_{\rm D}^3$	0 – 1	Benefit
I	$C_{\rm I}$	Maneuvering speed	$c_{\rm I}^1$	km/h	Benefit
		Damaging radius	$c_{\rm I}^2$	m	Benefit
		Striking accuracy	$c_{\rm I}^3$	0 – 1	Benefit
		Effective range	$c_{\rm I}^4$	km	Benefit
T	$C_{\rm T}$	Maneuvering speed	$c_{\rm T}^1$	km/h	Benefit
		Warning time	$c_{\rm T}^2$	s	Benefit
		Destructive capability	$c_{\rm T}^3$	0 – 1	Benefit
		Stealth capability	$c_{\rm T}^4$	0 – 1	Benefit
Communication	$C_{\rm C}$	Communication coverage	$c_{\rm C}^1$	km	Benefit
		Communication rate	$c_{\rm C}^2$	Mb/s	Benefit
		Communication capacity	$c_{\rm C}^3$	bit/s/Hz	Benefit
		Communication delay	$c_{\rm C}^4$	ms	Cost
		Communication quality	$c_{\rm C}^5$	0 – 1	Cost

To address the differences in units among various indicators and ensure comparability, normalization is necessary. In this paper, based on the extreme value processing method, a nonlinear dimensionless method is used to process the indicator values. Let c_i^j be the value of a capability indicator, $c_{i\max}^j$ and $c_{i\min}^j$ be the maximum and minimum values of the capability indicator, k be the function parameter determined by the utility interval.

If c_i^j represents a benefit-type capability indicator, the normalized value is expressed as follows:

$$\tilde{c}_i^j = \begin{cases} 1-\exp(-k\left(\left(\dfrac{c_{\rm i}^j - c_{i\min}^j}{c_{i\max}^j - c_{i\min}^j}\right)^2\right), & c_{\rm i\min}^j < c_i^j < c_{i\max}^j \\ 0, \ c_i^j < c_{\rm i\min}^j \end{cases}. \quad (1)$$

If c_i^j represents a cost-type capability indicator, the normalized value is expressed as follows:

$$\tilde{c}_i^j = \begin{cases} 1-\exp(-k\left(\left(\dfrac{c_{\rm i}^j}{c_{i\max}^j - c_{i\min}^j} - 1\right)^2\right), & c_{i\min}^j < c_i^j < c_{i\max}^j \\ 0, \ c_i^j \geqslant c_{i\max}^j \end{cases}. \quad (2)$$

2.2.2 Modeling of edges

The nodes interact with each other through the operation loop to establish the combat network of ASoS. There are four types of nodes in the functional layer, since some of the edge modes do not have actual combat significance or the probability of occurring in combat is extremely small, these edges are not taken into account. The analysis in this study focuses on six types of node edges, and the set of edges is L_{ij}, which can be expressed as

$$L_{ij} = \{L_{\rm T\to S}, L_{{\rm S}\to D}, L_{\rm S\to S}, L_{{\rm D}\to I}, L_{{\rm D}\to D}, L_{\rm I\to T}\}.$$

Table 2 explains how connecting edges of different functional nodes are connected based on their actual meaning.

Table 2 Six categories of edges

Edge type	Meaning
T → S	Intelligence acquisition
S → S	Intelligence sharing
S → D	Information uploading
D → D	Collaboration between decision
D → I	Fire control
I → T	Destroy enemy targets

The association relationship represented by the node edges is modeled based on the mutual transfer effect between the nodes. The value of each edge capacity is calculated using information entropy and evidence theory.

(i) Edge T → S. The T → S edge represents the directed edge from the target node to the reconnaissance node, established by the reconnaissance-type functional node to conduct reconnaissance on the target. This primarily involves considering the reconnaissance capability of the reconnaissance node and the counter-reconnaissance capability of the target node [40]. The value of the connected edge is calculated based on the reconnaissance class node’s discovery and recognition ability, tracking ability, and the target class’s hiding ability. The indicators involved are the indicator terms of the reconnaissance class and the target class connecting node. This can be expressed by

$$\begin{cases} c_{\rm T\text{-}S} = \exp(w_f \ln p_f + w_g \ln p_g) \\ p_f = k \cdot \dfrac{\exp\left(\displaystyle\sum_{j=1}^{n} \omega_{c_{\rm S}^j} \ln \tilde{c}_{\rm S}^j\right)}{\exp\left(\displaystyle\sum_{j=1}^{n} \omega_{c_{\rm T}^j} \ln \tilde{c}_{\rm T}^j\right)}, \quad p_f \in [0,1] \end{cases} \quad (3)$$

where p_f and p_g denote the discovery recognition capability and target tracking capability, respectively, $w_{c_i^j}$ is the weight value of the node capability index, and k is the environment correction parameter, which takes the value of 1 when the operation loop does not have any effect on the target reconnaissance.

(ii) Edge $\mathrm{I} \to \mathrm{T}$. The $\mathrm{I} \to \mathrm{T}$ edge is a directed edge that represents the strike class node sending combat commands to the target class node. The value of the connected edge is calculated based on the killing ability of the strike class node and the defense ability of the target class node, and can be expressed by the following:

$$c_{\text{I-T}} = k \cdot \frac{\exp\left(\sum_{j=1}^{n} \omega_{c_{\mathrm{I}}^j} \ln \tilde{c}_{\mathrm{I}}^j\right)}{\exp\left(\sum_{j=1}^{n} \omega_{c_{\mathrm{T}}^j} \ln \tilde{c}_{\mathrm{T}}^j\right)} \tag{4}$$

where $w_{c_i^j}$ denotes the weight value of the node capability index, and k is the environment correction parameter, which takes the value of 1 when the operation loop does not have any effect on the target reconnaissance.

(iii) The four classes of edges such as S-S, S-D, D-D, and D-I indicate the transmission and interaction of intelligence or decision-making information among nodes of sensor, decision, and influence classes. Therefore, they are categorized into the same class for calculation. Regarding the four classes of connected edge capabilities mentioned above, this study employs confidence interval to characterize their performance, accounting for node heterogeneity and inherent uncertainties in information interaction. Specifically, we establish belief rules for communication capability indicators (e.g., indicator c_{C}^i) between connected edges. The interval confidence measures are subsequently processed using the evidence reasoning (ER) method to derive the computed values of node-connected edges [41–43].

Assume that the node edge-connectivity computation consists of L mutually independent evidences between them, then the evidence can be expressed as follows:

$$e_i = \{(\theta, p_{\theta,i}); (\Theta, p_{\Theta,i})\} \tag{5}$$

where $p_{\theta,i}$ denotes the confidence with which evidence e_i, e_i is assessed as rank θ, and $p_{\Theta,i}$ denotes global ignorance.

Based on the above equation introduces the evidence weight and reliability, so that the weight of the evidence is ω_i, the reliability is r_i, then the form of the confidence distribution with weight and reliability can be expressed as

$$m_i = \{(\theta, \tilde{m}_{\theta,i}), \forall \theta \subseteq \Theta; (P(\Theta), \tilde{m}_{P(\Theta),i})\} \tag{6}$$

where $\tilde{m}_{\theta,i}$ denotes the reliability after the introduction of weights and reliability, which is calculated as

$$\tilde{m}_{\theta,i} = \begin{cases} 0, & \theta = \varnothing \\ c_{rw,i} m_{\theta,i}, & \theta \subseteq \Theta; \theta \neq \varnothing \\ c_{rw,i}(1 - r_i), & \theta = P(\Theta) \end{cases} \tag{7}$$

where $m_{\theta,i} = w_i p_{\theta,i}$; $c_{rw,i} = 1/(1 + w_i - r_i)$ is the normalization factor.

For two mutually independent evidence rules, the ER fusion rule method is utilized for combination processing, and the confidence value $p_{\theta,e(2)}$ after processing can be expressed by the following equation:

$$p_{\theta,e(2)} = \begin{cases} 0, & \theta = \varnothing \\ \dfrac{\hat{m}_{\theta,e(2)}}{\sum\limits_{C \subseteq \Theta} \hat{m}_{C,e(2)}}, & \theta \subseteq \Theta; \theta \neq \varnothing \end{cases}, \tag{8}$$

$$\hat{m}_{\theta,e(2)} = [(1 - r_i) m_{\theta,j} + (1 - r_j) m_{\theta,i}] + \sum_{A \cap B = \theta} m_{A,i} m_{B,j}, \ \forall \theta \subseteq \Theta, \tag{9}$$

where $\hat{m}_{\theta,e(2)}$ is the un-normalized confidence assigned to rank θ after the combination of the two pieces of evidence, A, B, and C all denote a certain subset.

2.3 Operation loop capability evaluation

The combat loop is directed. After obtaining the node boundary value, the capability value of a single combat loop is calculated, and the capability value of a single combat loop is defined as

$$E_{Li} = c_{\text{T-S}} \cdot c_{\text{S-D}} \cdot c_{\text{D-I}} \cdot c_{\text{I-T}}. \tag{10}$$

When there is a node-parallel structure in the operation loop, the same type of functional nodes have the same input and output nodes (Fig. 4). Connecting edges of the same functional nodes are assigned weights, which are obtained through an improved analytic hierarchy process, and then the value of the capability of the connecting edge under the parallel structure is

$$c'_{ij} = 1 - \prod_{j=1}^{n} (1 - \omega_{ij} c_{ij}) \tag{11}$$

where ω_{ij} denotes the weight of the node edge. The larger ω_{ij} is, the more important the edge is, where $0 < \omega_{ij} \leqslant 1$.

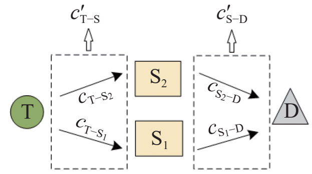

Fig. 4 Parallel structure of functional nodes

At this point, the value of the individual combat effectiveness of the operation loop changes to

$$E_{Li} = c'_{\text{T-S}} \cdot c'_{\text{S-D}} \cdot c_{\text{D-I}} \cdot c_{\text{I-T}}. \tag{12}$$

In the combat network, different equipment function nodes constitute several operation loops based on the target nodes and the relationship between the nodes and eventually form a heterogeneous combat network of equipment systems. For combat networks, expanding the scale of the combat system without optimizing its internal structure may lead to an increase in the number of nodes, resulting in redundancy. Consequently, the combat effectiveness may not improve proportionally with the increase in the number of operation loops. However, as long as the number of nodes in the combat network has not reached saturation, considering the heterogeneity of equipment and their associated relationships, a combat network with more operation loop exhibit higher effectiveness. Therefore, the capability value of the operation loop and the number of the operation loop are used in this paper to evaluate the combat effectiveness of ASoS.

Define $E_{C_{Ti}}$ as the combat effectiveness value for the target node C_{Ti}, which is given by

$$E_{C_{Ti}} = E_{L1} + \bar{E}_{L1}\left\{E_{L2} + \bar{E}_{L2}\left\{\cdots\left\{E_{L(m-1)} + \bar{E}_{L(m-1)}\left(E_{Lm}\right)\right\}\right\}\right\} \tag{13}$$

where m is the number of operation loops containing the target node C_{Ti}.

In general, a combat network comprises multiple target nodes that require attack. The weights of these target nodes are determined according to their respective importance levels and then aggregated to calculate the combat effectiveness value of the AsoS [44]:

$$E = \sum_{i=1}^{n} \omega_i E_{C_{Ti}} \tag{14}$$

where ω_i is the weight of the target node.

3. Contribution rate method based on the Shapley value

3.1 Contribution rate method based on the ratio

The RCR is the most commonly used method of calculating CRSoS and is shown in the following equation. Let equipment i be a certain type of equipment in the equipment system, the CRSoS of equipment i is

$$\text{CR}_i^x = \frac{E_1 - E_0}{E_0} \tag{15}$$

where E_1 denotes the combat effectiveness of the equipment system when equipment i is included, and E_0 denotes the combat effectiveness of the equipment system when equipment i is not included.

3.2 Contribution rate method based on improved Shapley value

Cooperative games investigate the issue of distributing benefits from a coalition perspective, emphasizing the importance of collaboration and collective interests. Common distribution methods include the kernel of the cooperative game, the egalitarian solution, and the Shapley value. Among them, the Shapley value distributes profits based on the marginal contribution of coalition members. This means that each participating member receives a benefit equal to the average of their marginal contribution to all coalitions. The Shapley value is characterized by properties such as validity and additivity [35].

The cooperative game is proposed as a research framework, the Shapley value model is introduced as the basis for calculating CRSoS, with the functional nodes in the equipment system considered coalition members. The combat effectiveness obtained through the operation loop is regarded as the gain, transforming the CRSoS issue into an optimal distribution problem of the gain within the cooperative game. By taking into account the interdependent relationships and synergy among the functional nodes of the ASoS, the calculation model of the CRSoS is constructed based on the Shapley value.

The classical Shapley value method is given as

$$\varphi_i(v) = \sum \omega(|s|)\left[v(s) - v(s/i)\right], \tag{16}$$

$$\omega(|s|) = \frac{(n-|s|)!\,(|s|-1)!}{n!}. \tag{17}$$

This paper makes the following definitions for the ASoS and the Shapley value model.

Definition 1 The functional layer of the ASoS comprises n functional nodes, where $N = (1, 2, \cdots, n)$ is the set of functional nodes of the ASoS, and s is a subset of N. $v(s)$ represents the combat effectiveness of the set s in the cooperative game. If $s = N$, then $v(s)$ denotes the value of the combat effectiveness of the ASoS that contains all the functional nodes in the ASoS.

Definition 2 Due to the role of correlation between equipment and between functional modules in a single piece of equipment, the number of nodes associated with a functional node is denoted as g. The total number of functional nodes after removing the g nodes is n' where $n' = g + 1$. Node i is combined with associated nodes to form a coalition of multiple functional nodes s, and the number of the coalition is $g(g+1)/2$. The value of the combat effectiveness of the coalition with node i included is $v(n' \cup s_i)$, and the value of the combat effectiveness of node i without nodes i included is $v(n' \cup (s_i/i))$.

Definition 3 $v(n' \cup s_i) - v(n' \cup (s_i/i))$ is defined as the change in the effectiveness of the set before and after the functional node i joins the functional node alliance s_i. The weight factor of a functional node under different functional node alliances is denoted by $\omega(|s_i|)$.

Based on the above, the CRSoS of a functional node i in the set s is

$$\mathrm{CR}_i^s = \frac{\varphi_i(v)}{v(N)} = \frac{\sum\limits_{i \in s_i} \omega(s_i)[v(n' \cup s_i) - v(n' \cup (s_i/i))]}{v(N)}. \quad (18)$$

However, the classical Shapley value method distributes the benefits according to the marginal contribution of the coalition members. This method assumes equal influence of each functional node on the allocation of operational effectiveness and overlooks factors that indirectly affect the distribution of operational effectiveness. Therefore, this paper includes the non-effectiveness factors that are not involved in combat effectiveness between nodes of the same functional type in combat, such as node reliability, security, and environmental adaptability, in the scope of model consideration, and introduces the improvement factor Δm_i to adjust the CRSoS of the nodes.

Let $G_i = (g_i^1, g_i^2, g_i^3)$ be the set of data normalized to non-efficacy influences, such as node reliability, safeguard, and environmental adaptability. The degree of influence of these factors is then determined.

$$m_i = \begin{bmatrix} g_i^1 & g_i^2 & g_i^3 \end{bmatrix} \begin{bmatrix} \eta_1 / \sum\limits_{i=1}^{k} g_i^1 \\ \eta_2 / \sum\limits_{i=1}^{k} g_i^2 \\ \eta_3 / \sum\limits_{i=1}^{k} g_i^3 \end{bmatrix} \quad (19)$$

where $\eta_j (j = 3)$ is the weight coefficient of the influencing factors and k is the number of nodes of the same type [44,45].

The mean value of the influence factor g_i^j under the same type of node is represented by

$$\bar{g}_i^j = \frac{1}{k} \sum_{i=1}^{k} g_i^j. \quad (20)$$

The mean square error of the influence factor g_i^j under the same type of node is represented by

$$s_{g_i^j} = \left(\frac{1}{k} \sum_{i=1}^{k} \left(g_i^j - \bar{g}_i^j \right)^2 \right)^{\frac{1}{2}}, \quad (21)$$

$$\varphi_{g_i^j} = \bar{g}_i^j / s_{g_i^j}. \quad (22)$$

Then n_j can be expressed as

$$\eta_j = \frac{\varphi_{g_i^j}}{\sum\limits_{j=1}^{3} \varphi_{g_i^j}}. \quad (23)$$

The final improvement factor can be expressed as

$$\Delta m_i = m_i - 1/k. \quad (24)$$

After introducing the improvement factor, the allocation is made quadratically based on the Shapley value. The allocation correction can then be expressed as

$$\tilde{\varphi}_i(v) = \varphi_i(v) + \Delta m_i \cdot \sum_{i=1}^{k} \varphi_i(v). \quad (25)$$

At this point, the CRSoS $\overline{\mathrm{CR}_i^s}$ of a functional node i in set s, under the contribution rate method based on improved Shapley value is

$$\overline{\mathrm{CR}_i^s} = \frac{\tilde{\varphi}_i(v)}{v(n)}. \quad (26)$$

4. Case study

To demonstrate the soundness and scientific validity of the OLISV in CRSoS assessment, an urban warfare case is considered and the information to be entered for this case is provided. Finally, the results are analyzed, leading to some meaningful conclusions are drawn.

4.1 Case description

Take the example of a red side infantry squad performing the urban building clearance mission. The equipment in the infantry squad is mapped and decomposed into corresponding functional nodes according to "one-to-one" and "one-to-many" principles, and finally, a multi-layer network model of ASoS has been constructed. The model comprises the operational task layer, equipment layer, and functional node layer, as shown in Fig. 5. The equipment entities at the equipment layer are categorized into the human-machine cooperative system, the solid system, and the unmanned system. The human-machine cooperative system includes equipment C^3S_2, C^3S_3, and C^3S_4, the unmanned system includes equipment UE_1, UE_2, UE_4, UE_5, and UE_6, and the solider system encompasses the remaining equipment.

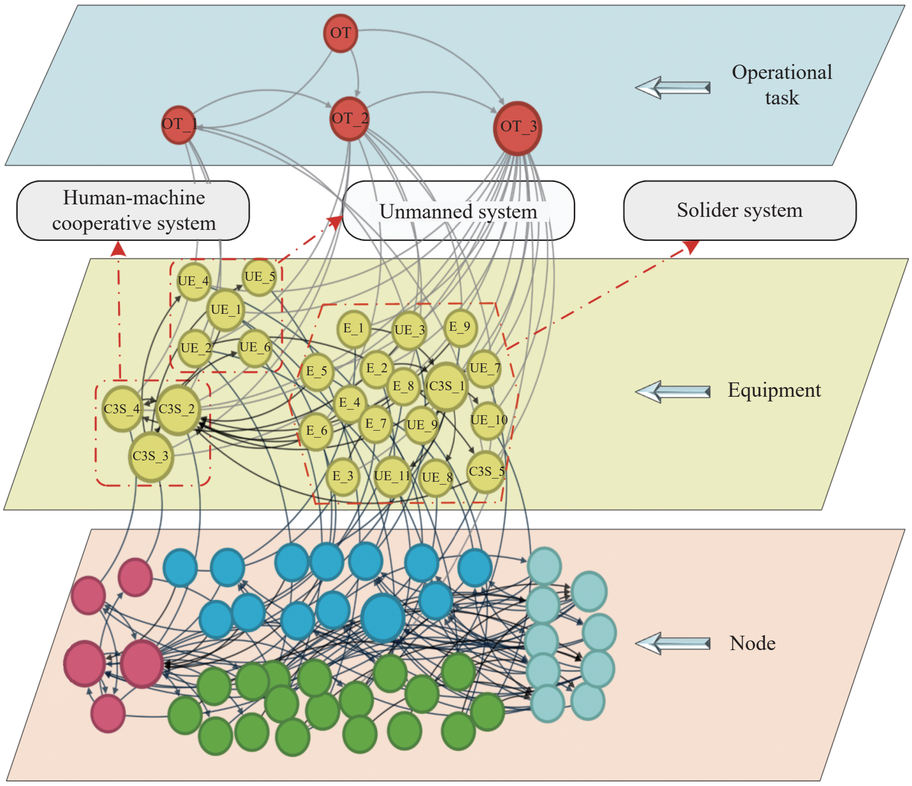

Fig. 5 Operational task-equipment-functional node network model

Fig. 6 shows the functional node layer network of the ASoS. The functional node layer contains 45 nodes, of which the number of target nodes is 9, the number of sensor nodes is 13, the number of decision nodes is 5, and the number of influence nodes is 18. Moreover, there are a total of 25 types of equipment corresponding to the ASoS, of which there are 11 unmanned equipment, 9 manned equipment, and 5 collaborative accusation systems.

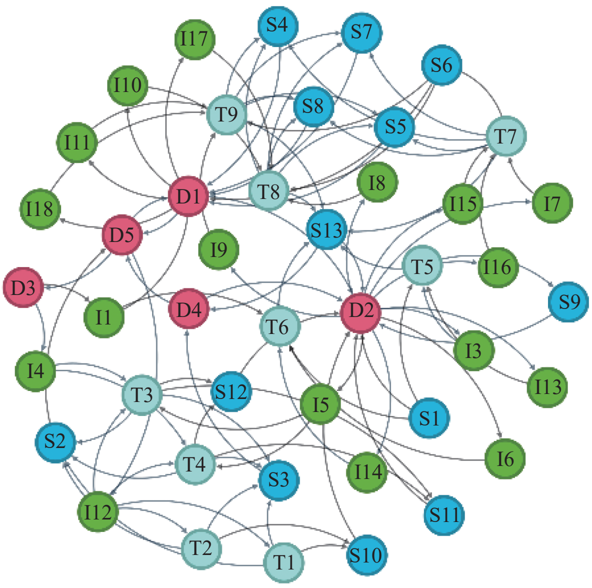

Fig. 6 Functional nodes network

Table 3 provides a detailed correspondence between the equipment and their respective functional nodes. The quantity of equipment with a single function is 14, and the quantity of equipment with multiple functional is 11.

Table 3 Correspondence between functional nodes and equipment

Functional nodes	Equipment	Functional nodes	Equipment	Functional nodes	Equipment
S_1 I_3	UE_1	S_9 I_{14}	E_6	S_8 I_{11}	E_5
S_2 I_{12}	UE_2	S_{10} I_6	E_7	S_3 D_5	UE_3 C^3S_5
S_4 I_8	E_1	S_{11} I_5	E_8	I_1 I_2	UE_4 UE_5
S_5 I_9	E_2	S_{12} I_{13}	E_9	I_4 I_{15}	UE_6 UE_7
S_6 I_{10}	E_3	D_1 D_2	C^3S_1 C^3S_2	I_{16} I_{17}	UE_8 UE_9
S_7 I_7	E_4	D_3 D_4	C^3S_3 C^3S_4	I_{18} S_{13}	UE_{10} UE_{11}

The urban building clearance mission is divided into three phases based on the mission decomposition theory, with operational task phase 1 consisting mainly of unmanned equipment attacking enemy targets outside the building after battlefield reconnaissance is completed, operational task phase 2 focuses on long-range precision strikes, and roof strikes against exposed enemy targets. Operational task phase 3 centers on sensing and clearing the enemy targets inside the building. The operation loops formed against different enemy targets are shown in Fig. 7.

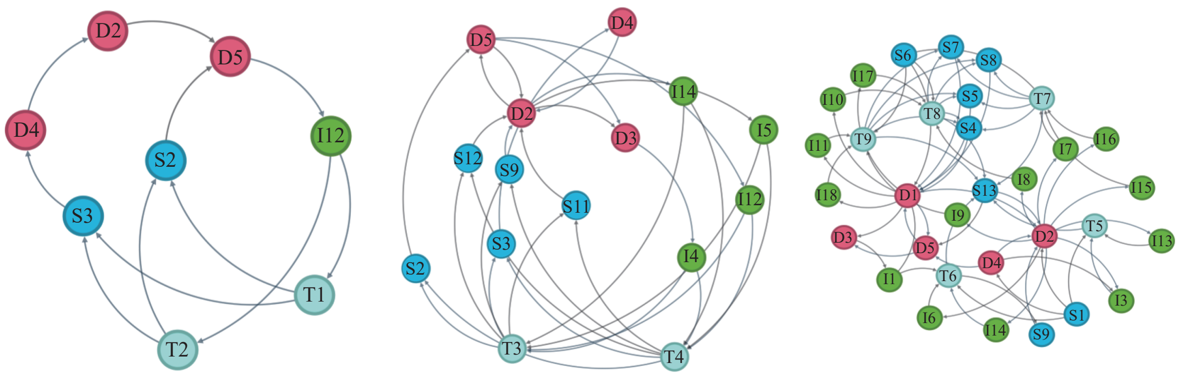

(a) Operational task phase 1 (b) Operational task phase 2 (c) Operational task phase 3

Fig. 7 Operation loop under different phases

The effectiveness of each operation loop and the combat effectiveness of the ASoS are calculated for enemy targets in the operation loop. The example contains 96 operation loops. Due to space limitations, only the following loops and their corresponding combat effectiveness values are listed in this paper, as shown in Table 4.

Table 4 Combat effectiveness of the operation loop

Number	Operation loop	Combat effectiveness
1	$T_3 \to S_2 \to D_5 \to D_2 \to D_5 \to I_{12} \to T_3$	0.265
2	$T_3 \to S_2 \to D_5 \to D_2 \to D_3 \to I_4 \to T_3$	0.271
3	$T_3 \to S_2 \to D_5 \to I_5 \to T_3$	0.318
4	$T_3 \to S_3 \to D_4 \to D_2 \to D_3 \to I_4 \to T_3$	0.288
5	$T_3 \to S_3 \to D_4 \to D_2 \to I_5 \to T_3$	0.336
6	$T_3 \to S_3 \to D_4 \to D_2 \to D_5 \to I_{12} \to T_3$	0.292
⋮	⋮	⋮
96	$T_9 \to S_{13} \to D_5 \to D_1 \to I_{16} \to T_9$	0.294

4.2 Analysis of experimental results

4.2.1 Analysis of the CRSoS of functional nodes and equipment under the sub-task phase

By employing three different calculation methods discussed earlier, the CRSoSs of functional nodes at various phages of tasks are determined. Then, based on the one-to-one and one-to-many relationships between equipment and nodes, the CRSoSs of the nodes are summed to obtain the CRSoS of the equipment.

(i) Operational task phase 1

Table 5 shows the CRSoS for the functional nodes under operational task phase 1 and Fig. 8 shows the CRSoS for the functional nodes and equipment. It can be seen that for both nodes S_3, S_2, D_4 D_2, the results calculated using the Shapley value contribution rate (SCR) method are much larger than the SCR method. Redistribution of results using the ISCR method, further considering the role of the node's non-effectiveness factors, the change rate of sensor nodes is approximately 2%. For both nodes D_5 and I_{12}, the CRSoS can not be derived due to the limitations of the RCR method; using the SCR method it is calculated as 1, i.e., the system contribution of nodes D_5 and I_{12} in operational task phase 1 is 100%, which proves that the node is indispensable in ASoS. After the aggregation calculation, the CRSoS of the unmanned equipment UE_2 is the highest, followed by the collaborative accusation systems C^3S_5. The CRSoS of the remaining equipment is the same. This is because unmanned equipment UE_2 consists of two nodes S_2 and I_{12} and the rest of the equipment corresponds to the nodes one by one, which reduces the CRSoS of equipment C^3S_5 corresponding to the node D_5 after normalization.

Table 5 CRSoS under phase 1 of the operational task

Node number	RCR	SCR	ISCR	Change rate/%
S_3	0.7737	0.2181	0.2223	1.9
S_2	0.6644	0.1996	0.1954	−2.1
D_4	0.7737	0.2181	0.2184	0.1
D_2	0.7737	0.2181	0.2176	−0.2
D_5	–	1	1	0.0
I_{12}	–	1	1	0.0

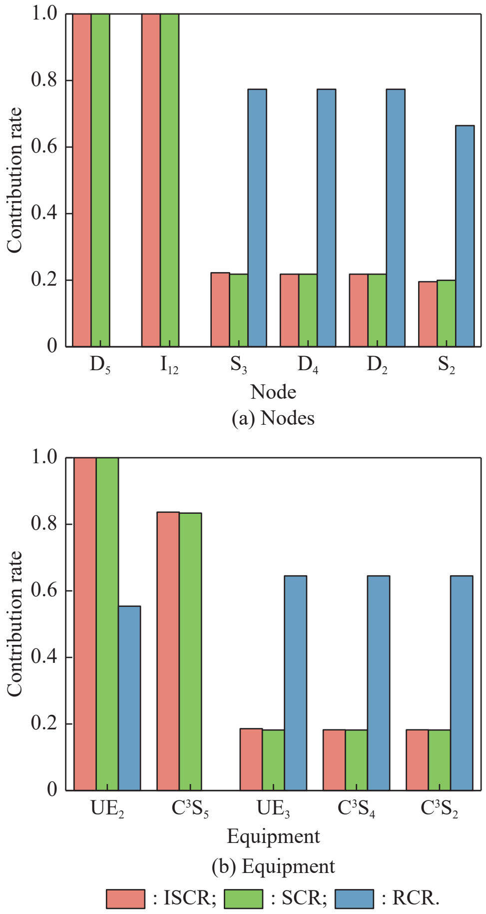

Fig. 8 Comparison of CRSoS under phase 1 of the operational task

(ii) Operational task phase 2

Table 6 shows the CRSoS values for the functional nodes under operational task phase 2 and Fig. 9 shows the CRSoS for the functional nodes and equipment. It can be seen that for both sensor and influence nodes, the results calculated using the RCR method are greater than the SCR method, the reason is that when calculating the sensor and influence nodes, due to the existence of a dependency relationship between the associated nodes, when the dependent nodes fail, the target nodes also fail, making the results of the SCR calculation method smaller. Contrarily, the decision nodes in the combat network have the characteristics of substitution and mutual independence, which makes the CRSoS of the decision nodes calculated by the SCR method larger than that of the RCR method.

Table 6 CRSoS under phase 2 of the operational task

Node number	RCR	SCR	ISCR	Change rate/%
D_2	0.1946	0.4058	0.4178	2.9
D_5	0.1469	0.1802	0.1755	−2.6
D_3	0.0586	0.1124	0.1095	−2.5
D_4	0.0483	0.0756	0.0710	−6.2
S_2	0.0565	0.0331	0.0323	−2.6
I_{12}	0.0540	0.0316	0.0309	−2.2
S_3	0.0637	0.0299	0.0291	−2.9
I_4	0.0574	0.0272	0.0264	−2.6
I_5	0.0285	0.0138	0.0148	7.2
S_9	0.0252	0.0123	0.0125	1.7
S_{11}	0.0188	0.0092	0.0100	8.1
S_{12}	0.0188	0.0092	0.0100	8.1
I_{14}	0.0104	0.0061	0.0066	6.9

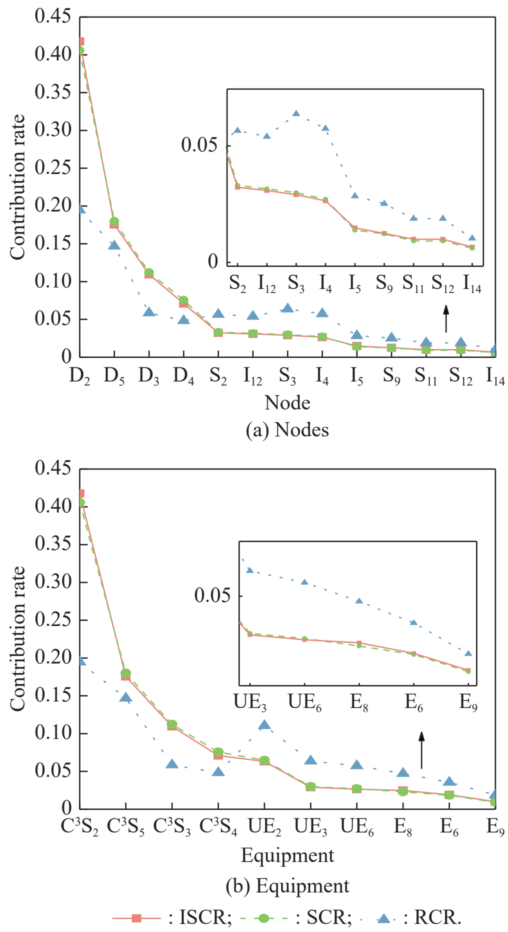

Fig. 9 Comparison of CRSoS under phase 2 of the operational task

Further redistribution of the CRSoS of the nodes using the ISCR method improves the CRSoS of nodes S_9, S_{11}, S_{12}, D_2, I_5, and I_{14}. This is because nodes S_9, S_{11}, S_{12}, D_2, I_5 have better reliability, security, and environmental adaptability than their counterparts, which in turn increases their CRSoS by the improvement factor. The change rate for most nodes is approximately 3%, while the change rate of a few nodes is around 8%. Furthermore, the observed higher rate of change for sensors node in operational task phase 2 can be attributed to three primary factors: (i) A significant increase in the number of deployed sensor nodes compared to operational task phase 1. (ii) The number of manned over unmanned sensor nodes. (iii) The demonstrated superior performance characteristics of manned sensor nodes in terms of reliability, security, and environmental adaptability.

The CRSoS of the nodes under the RCR and ISCR methods are ranked separately and the importance of nodes S_3, S_2, D_3, D_4, I_4, and I_{12} is different under the two methods. The ISCR method increases the importance of the decision nodes and readjusts the order of nodes S_3, S_2, I_4, and I_{12}. Compared to the SCR method, the ISCR method does not alter the ranking of nodes. The result is more valid.

Rank the CRSoS of the nodes according to the RCR method:

$$D_2 \succ D_5 \succ S_3 \succ D_3 \succ I_4 \succ S_2 \succ I_{12} \succ$$
$$D_4 \succ I_5 \succ S_9 \succ S_{11} \succ S_{12} \succ I_{14}.$$

Rank the CRSoS of the nodes according to the SCR method:

$$D_2 \succ D_5 \succ D_3 \succ D_4 \succ S_2 \succ I_{12} \succ$$
$$S_3 \succ I_4 \succ I_5 \succ S_9 \succ S_{11} \succ S_{12} \succ I_{14}.$$

Rank the CRSoS of the nodes according to the ISCR method:

$$D_2 \succ D_5 \succ D_3 \succ D_4 \succ S_2 \succ I_{12} \succ$$
$$S_3 \succ I_4 \succ I_5 \succ S_9 \succ S_{11} \succ S_{12} \succ I_{14}.$$

The trend in the CRSoS contribution of the equipment under the three methods is similar to that of the functional nodes, with the collaborative accusation systems C^3S_2 having the highest CRSoS of 41.8%, and unmanned equipment UE_2 in the unmanned equipment having a higher CRSoS of 6.3%.

(iii) Operational task phase 3

Table 7 shows the CRSoS values for the functional nodes under operational task phase 3 and Fig. 10 shows the CRSoS for the functional nodes and equipment. The results calculated using the RCR method are greater than those calculated using the SCR and ISCR methods, which are different from those of the decision functional nodes in operational task phase 2. The reason for this is that in operational task phase 3 there are fewer transfer relationships between decision nodes, the operation loop is simple, and it is mostly composed of individual sensor, decision, and influence nodes.

Table 7 CRSoS under phase 3 of the operational task

Node number	RCR	SCR	ISCR	Change rate/%	Node number	RCR	SCR	ISCR	Change rate/%
D_1	0.5588	0.2039	0.2114	3.7	S_8	0.0303	0.0147	0.0155	5.7
D_4	0.2219	0.1375	0.1323	−3.8	I_{14}	0.0276	0.0134	0.0136	1.5
S_1	0.1014	0.0985	0.0964	−2.1	I_{13}	0.0249	0.0121	0.0127	4.3
D_5	0.1939	0.0958	0.0906	−5.4	I_7	0.0209	0.0102	0.0107	5.1
D_2	0.0999	0.0773	0.0848	9.7	I_8	0.0182	0.0090	0.0095	5.8
S_{13}	0.1939	0.0812	0.0792	−2.5	I_9	0.0182	0.0090	0.0095	5.8
D_3	0.0511	0.0433	0.0386	−10.8	I_{10}	0.0182	0.0090	0.0095	5.8
I_1	0.0511	0.0243	0.0239	−1.8	I_{11}	0.0182	0.0090	0.0095	5.8
I_3	0.0539	0.0228	0.0224	−1.9	I_{15}	0.0169	0.0083	0.0076	−8.9
S_9	0.0441	0.0211	0.0210	−0.6	I_{16}	0.0169	0.0083	0.0076	−8.9
S_4	0.0303	0.0147	0.0155	5.7	I_{17}	0.0143	0.0070	0.0063	−10.6
S_5	0.0303	0.0147	0.0155	5.7	I_{18}	0.0143	0.0070	0.0063	−10.6
S_6	0.0303	0.0147	0.0155	5.7	I_6	0.0090	0.0045	0.0050	11.6
S_7	0.0303	0.0147	0.0155	5.7					

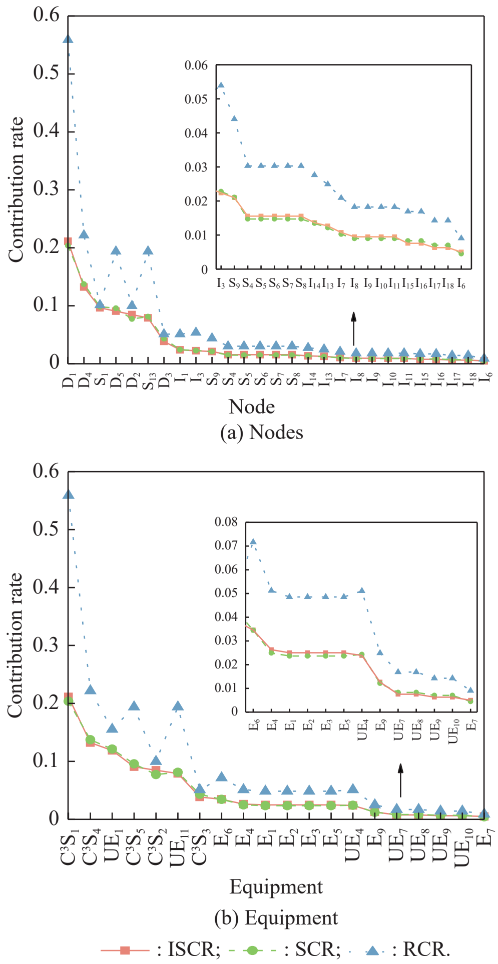

(a) Nodes

(b) Equipment

Fig. 10 Comparison of CRSoS under phase 3 of the operational task

The change rate for decision nodes D_2 and D_3 in phase 2 is typically around 3%. In phase 3, the change rate for D_2 and D_3 increases to approximately 10%. This difference is attributed to node D_2 being a manned decision system, while node D_3 is an unmanned collaborative software. The reliability and environmental adaptability of node D_3 are lower than those of node D_2. The reasons for targeting influence nodes such as I_6, I_{17}, and I_{18} are similar, while most other nodes exhibit a change rate of around 6%. Compared to the SCR method, the ISCR method alters the ranking relationship between nodes D_2 and S_{13}, with significant changes observed in some decision nodes and influence nodes.

Rank the CRSoS of the nodes according to the RCR method:

$$D_1 > D_4 > S_{13} > D_5 > S_1 > D_2 > I_3 > D_3 > I_1 > S_9 > S_4 > S_5 > S_6 > S_7 > S_8 > I_{14} > I_{13} > I_7 > I_8 > I_9 > I_{10} > I_{11} > I_{15} > I_{16} > I_{17} > I_{18} > I_6.$$

Rank the CRSoS of the nodes according to the SCR method:

$$D_1 > D_4 > S_1 > D_5 > S_{13} > D_2 > D_3 > I_1 > I_3 > S_9 > S_4 > S_5 > S_6 > S_7 > S_8 > I_{14} > I_{13} > I_7 > I_8 > I_9 > I_{10} > I_{11} > I_{15} > I_{16} > I_{17} > I_{18} > I_6.$$

Rank the CRSoS of the nodes according to the ISCR method:

$$D_1 > D_4 > S_1 > D_5 > D_2 > S_{13} > D_3 > I_1 > I_3 > S_9 > S_4 > S_5 > S_6 > S_7 > S_8 > I_{14} > I_{13} > I_7 > I_8 > I_9 > I_{10} > I_{11} > I_{15} > I_{16} > I_{17} > I_{18} > I_6.$$

The trend in the CRSoS of the equipment under the three methods is similar to that of the functional nodes, with the collaborative accusation systems C^3S_1 having the highest CRSoS of 21.1%, the unmanned equipment UE_1 in the unmanned equipment having a higher CRSoS of 11.9%, and manned equipment E_6 in the manned equipment having a higher CRSoS of 3.5%.

4.2.2 Analysis of the CRSoS of functional nodes and equipment under the whole operational task

The relative importance of different operational task phases is expressed in terms of weights, which are obtained through expert assignment. Subsequently, the CRSoSs of functional nodes and equipment under the whole mission are determined through weighted aggregation. As shown in Fig. 11 and Fig. 12, it can be seen that the CRSoS of the decision node is relatively high, and the CRSoS of I_{12} influence nodes is more prominent than that of other influence nodes. The reason is that the node I_{12} plays a major role in the operational task phases 1 and 2 and is the main influence node in the combat network.

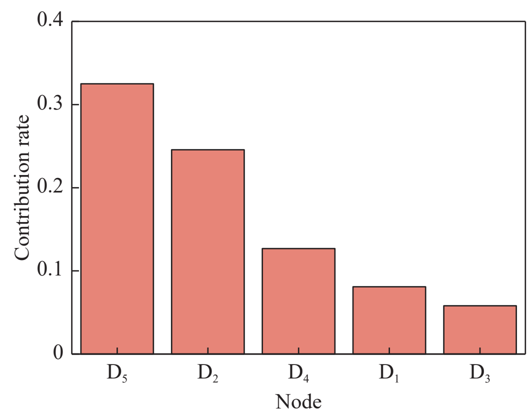

(a) Decision nodes

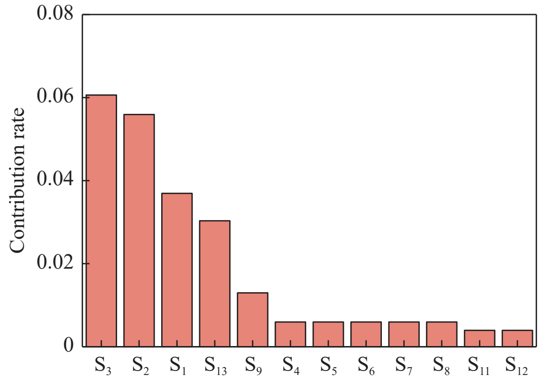

(b) Sensor nodes

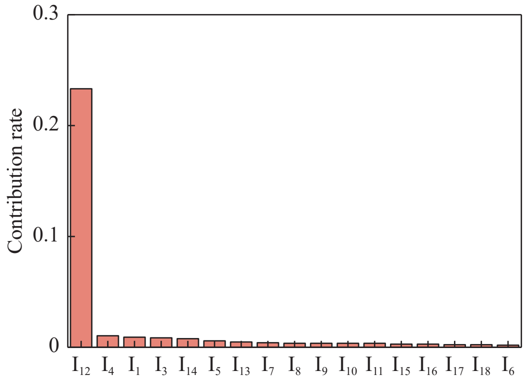

(c) Influence nodes

Fig. 11 CRSoS of the node under the whole operational task

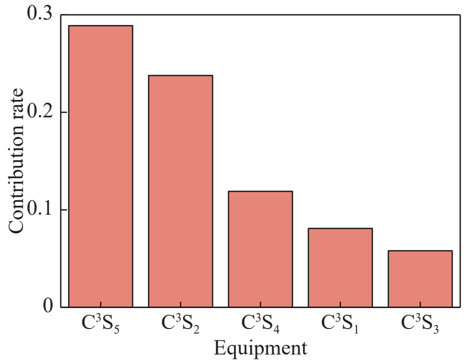

(a) Collaborative accusation system

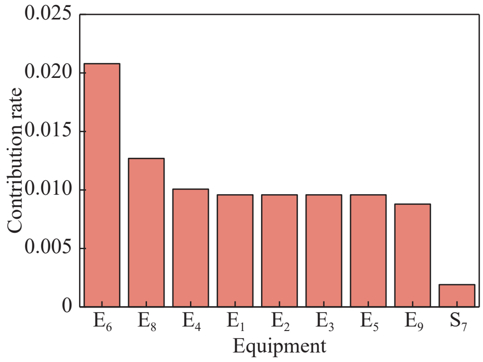

(b) Manned equipment

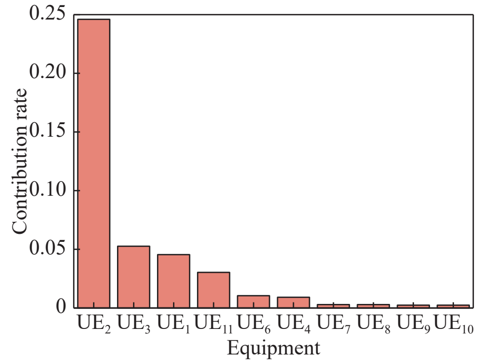

(c) Unmanned equipment

Fig. 12 CRSoS of the equipment under the whole operational task

In the ASoS, the collaborative accusation system generally plays a significant role, followed by unmanned equipment. This is because the collaborative accusation system is at the heart of the AsoS in combat. When the collaborative accusation system is disrupted, the mission may not be completed or even collapse. Meanwhile, unmanned equipment replaces manned equipment in combat, becoming the primary contributor to combat effectiveness.

Additionally, three decision nodes D_2, D_4, D_5 are taken as the target, and their CRSoS are analyzed under the three operational task phases. The results are as follows. Node D_5 has the largest CRSoS when it is at operational task phase 1 and the smallest CRSoS when it is at operational task phase 3, with a CRSoS of 0.091. Node D_2 has the highest CRSoS of 0.418 in operational task phase 2 and the lowest CRSoS of 0.082 in operational task phase 3. Node D_4 has the maximum CRSoS at task phase 1 with a value of 0.218 and the minimum CRSoS at task phase 2 with a value of 0.071.

The reason for the above results is that the same node has different positions in the combat network when it is in different combat phases. During operational task phase 1, the number of nodes is limited, and the node D_5 holds a key position in the combat network, resulting in a high CRSoS. However, during operational task phase 2, the node D_2 transitions into a more prominent role, alongside an expansion in the number of nodes, causing a reduction in the CRSoS of the node D_5.

4.2.3 Impact analysis of edge capability on combat effectiveness

The single-factor sensitivity test method is employed to assess the impact of edge capability on the operational effectiveness of ASoS during various task phases. Additionally, the sensitivity magnitude of edge-connecting capability is determined using differential calculation.

The formula for calculating sensitivity S is as follows:

$$S = \frac{\Delta E}{\Delta C} \tag{27}$$

where ΔE is incremental to combat effectiveness, and ΔC is the value of the change in the ability to edges.

The results are shown in Fig. 13, Fig. 14, and Fig. 15. It can be seen that the edge capability is positively correlated with the combat effectiveness of the ASoS in different phases of the operational task. In operational task phase 1 and operational task phase 2, the edges that have a greater impact on the combat effectiveness of the ASoS correspond to the nodes that have a greater CRSoS. For example, in the operational task phase 1, connecting edges D_2-D_5, D_5-I_{12}, and $I_{12}-T$ have a greater impact on combat effectiveness and the sensitivity coefficients are higher, with values of 0.658, 0.577, and 0.545 respectively. The rest of the connecting edges are smaller, corresponding to the larger nodes D_5 and I_{12} in the CRSoS analysis. However, in operational task phase 3, the changes in the capabilities of company edges such as D_4-D_2, D_4-I_3, and D_5-D_1 have a greater impact on the combat effectiveness of ASoS, and the sensitivity coefficients are higher, with values of 0.209, 0.141, and 0.152 respectively, which is different from the CRSoS analysis, where the nodes of D_1 and S_1 have a higher CRSoS than those of D_4 and S_{13}. This is because there are more operation loops containing decision nodes D_1 than node D_4 in task phase 3. However, the change in the capacity of a single connecting edge containing nodes D_4 and S_{13} has a higher impact on combat effectiveness than nodes D_1 and S_1.

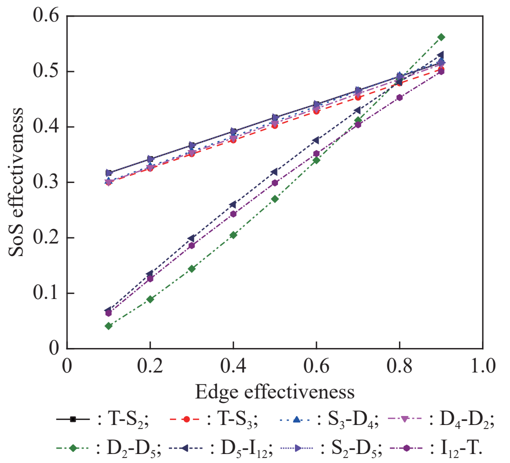

(a) Change in edge capability v.s. combat effectiveness

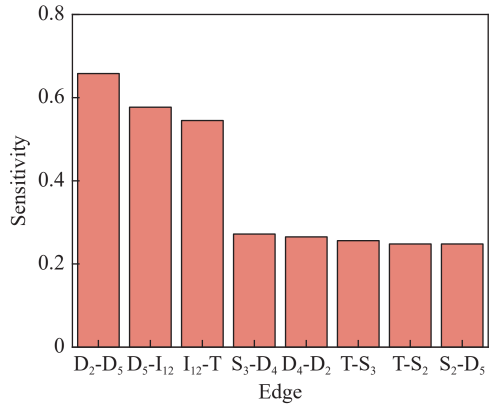

(b) Sensitivity factor for the edge

Fig. 13 Edge capability on combat effectiveness under operational task phase 1

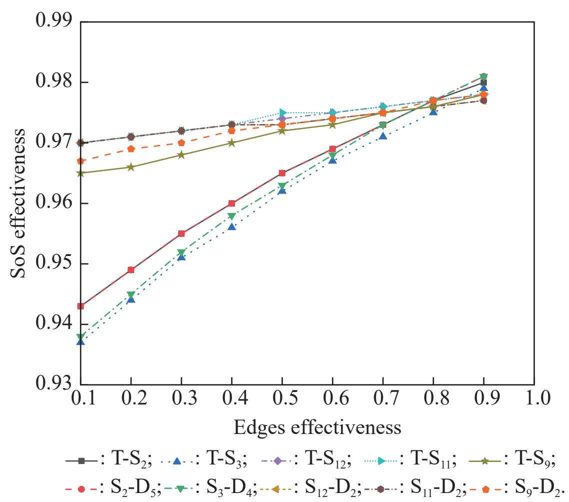

(a) Variation of sensor-type edge capability with combat effectiveness

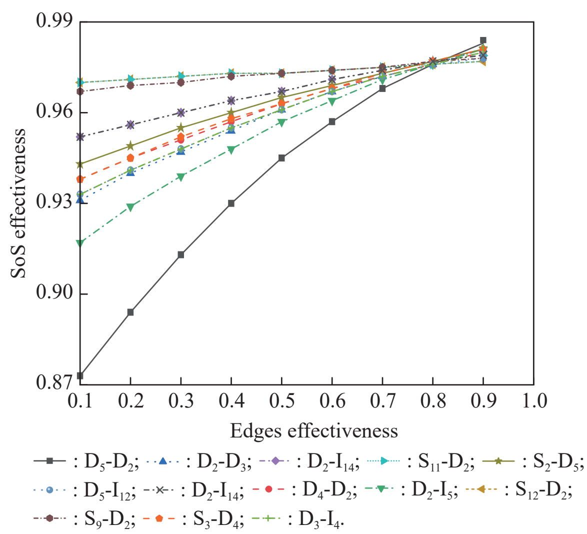

(b) Variation of decide-type edge capability with combat effectiveness

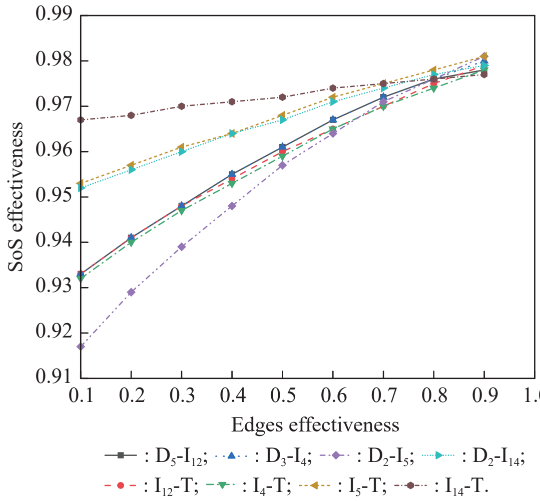

(c) Variation of influence-type edge capability with combat effectiveness

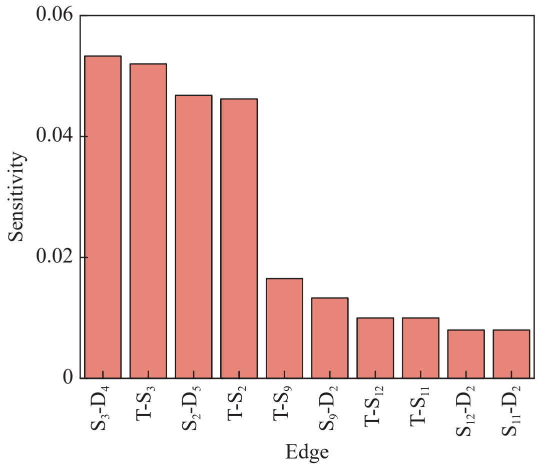

(d) Sensitivity factor for the sensor-type edge

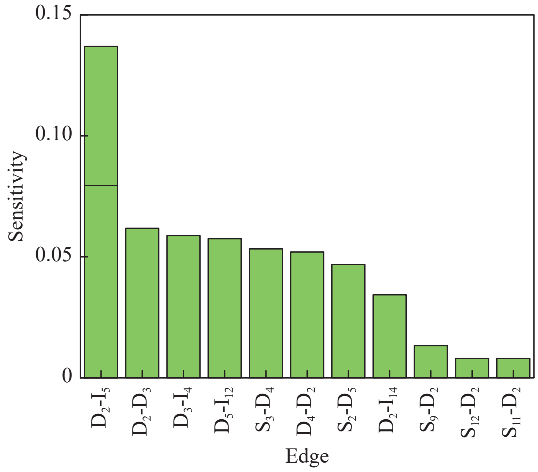

(e) Sensitivity factor for the decide-type edge

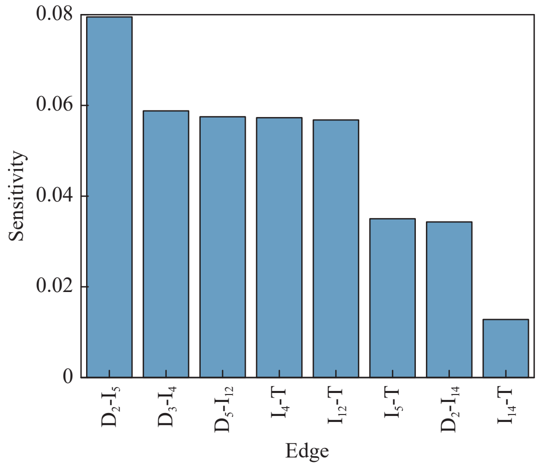

(f) Sensitivity factor for the influence-type edge

Fig. 14 Impact of edge capability on combat effectiveness under operational task phase 2

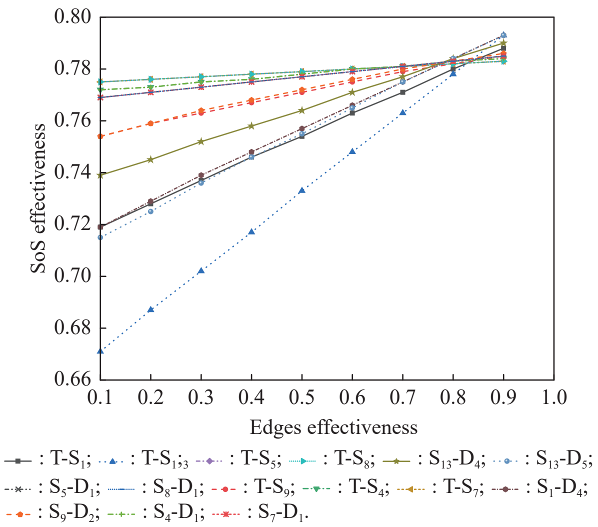

(a) Variation of sensor-type edge capability with combat effectiveness

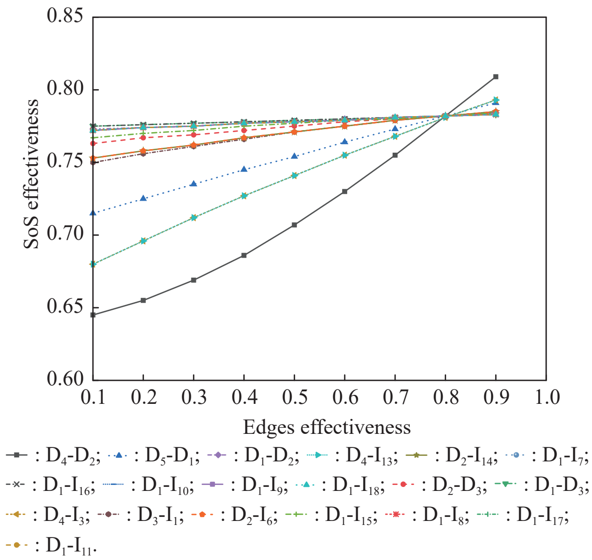

(b) Variation of decide-type edge capa-bility with combat effectiveness

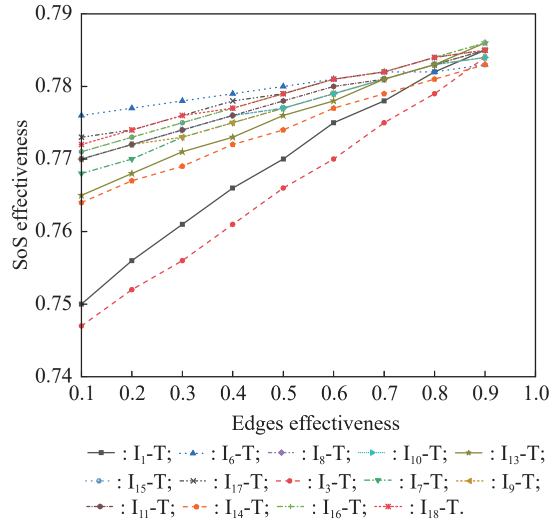

(c) Variation of influence-type edge capability with combat effectiveness

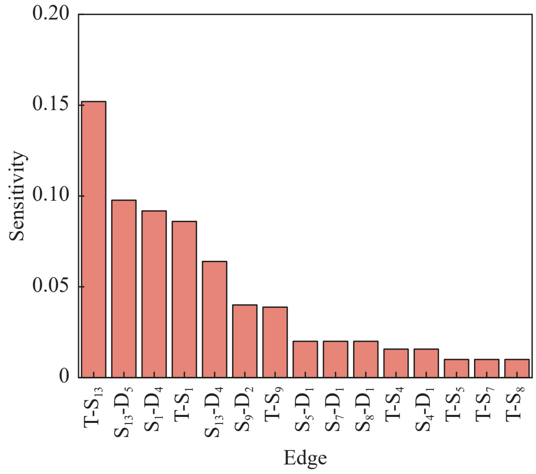

(d) Sensitivity factor for the sensor-type edge

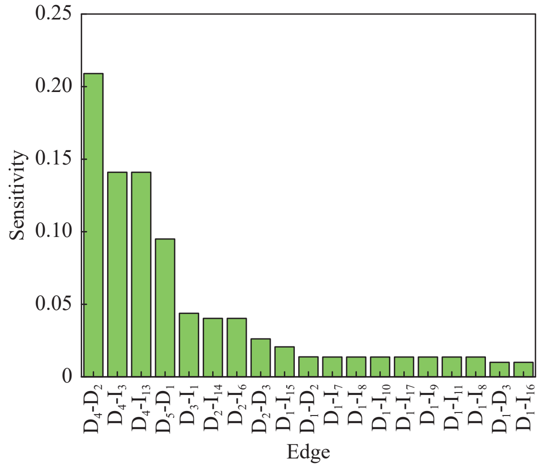

(e) Sensitivity factor for the decide-type edge

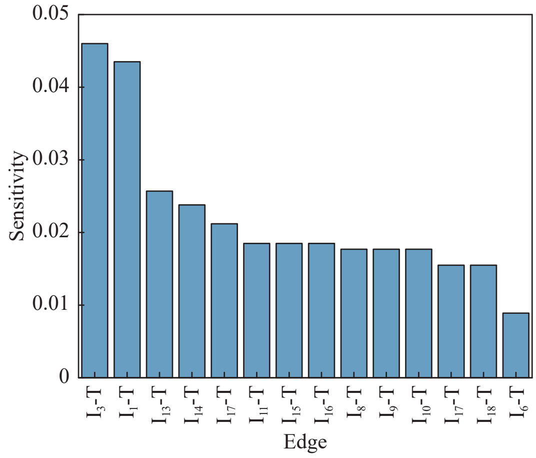

(f) Sensitivity factor for the influence-type edge

Fig. 15 Impact of edge capability on combat effectiveness under operational task phase 3

4.3 Results discussions

Based on the analysis of the above results, we make the following recommendations.

(i) In the infantry squad ASoS, the CRSoS of the collaborative accusation system is high, with unmanned equipment generally making a greater contribution than manned equipment in combat. For the future squad ASoS, It is essential to enhance the intelligent capability of the collaborative accusation system and increase the proportion of unmanned equipment within the squad ASoS, thus improving the overall intelligence level of infantry squads and meeting operational requirements.

(ii) CRSoS is dynamic and not a fixed value, which varies depending on the position of functional nodes during different phases of operational tasks, as well as their interactions with other nodes. In actual combat, it is generally believed that there should not be a situation where the CRSoS of a particular node is too large, as this would lead to the inability to complete an operational task if that specific node is to be destroyed. Consequently, the structure of the combat network should be modified accordingly to increase the number of nodes of the same type and reduce the CRSoS of that node.

(iii) The combat effectiveness of ASoS is positively correlated with the connecting edge capability, as indicated by the analysis results. In the event of damage to the combat network requiring repair, prioritizing the connecting edges with larger sensitivity coefficients is essential to swiftly enhance combat effectiveness. Therefore, it is recommended that the sensitivity coefficient of the connecting edges be used as the target for effective repair strategies.

5. Conclusions

In response to the problems in the evaluation of CRSoS, such as the inability of the RCR method to handle situations with zero combat effectiveness, do not take into account the correlation between equipment, and failure to decompose the evaluation object into functional modules of equipment, a framework called OLISV is proposed. The OLISV constructs the ASoS combat network by multi-layer heterogeneous network and operation loop methods and then obtains the CRSoS of functional nodes and equipment in the combat network by the improved Shapley value method. The case study analyzes the CRSoS of functional nodes and their corresponding equipment across various operational task phases, examining the impact of alterations in edge capabilities on combat effectiveness. The comparative results indicate that our proposed ISCR method can effectively address the influence of dependencies and correlations between nodes on CRSoS compared to the RCR method, and the ISCR method is more reasonable and scientific.

OLISV has the following merits.

(i) The OLISV takes into account synergies and dependencies between functional nodes and introduces non-effectiveness influencing factors to enhance the accuracy and reasonability of the CRSoS analysis results. In contrast, the RCR method calculates the CRSoS of a functional node by attributing changes in combat effectiveness to that node, disregarding the correlation between functional nodes.

(ii) The ISCR method addresses the issue that the RCR method cannot calculate the CRSoS of a functional node when its combat effectiveness becomes 0 after the node is removed, demonstrating that the ISCR method has a broader range of application scenarios.

(iii) A three-layer network model of the operational task, equipment, and functional nodes is constructed by adopting multilayer network modeling, and the CRSoS research objective is focused on the functional nodes within this model. The empowerment calculation is carried out for the parallel node structure in the combat network.

There is still much work to be done in the future, for example, further analysis on the impact of equipment performance parameters on CRSoS, the dynamic changes in equipment capabilities in a temporal combat network, and the optimization and design of the structure of the ASoS combat network.

References

[1] LI J C, ZHAO D L, JIANG J, et al. Capability oriented equipment contribution analysis in temporal combat networks. IEEE Trans. on Systems, Man, and Cybernetics: Systems, 2021, 51(2): 696–704.

[2] LI J C, GE B F, JIANG J, et al. High-end weapon equipment portfolio selection based on a heterogeneous network model. Journal of Global Optimization, 2020, 78(4): 743–761.

[3] HAN Q, PANG B, LI S, et al. Evaluation method and optimization strategies of resilience for air & space defense system of systems based on kill network theory and improved self-information quantity. Defence Technology, 2023, 21: 219–239.

[4] LI X B, WANG W P, LIN M, et al. The research framework, progress, and key directions of system-of-systems contribution ratio evaluation. Systems Engineering-Theory & Practice, 2019, 39(6): 1623–1634. (in Chinese)

[5] ZHOU C, SONG B F, SHANG B L, et al. System of systems contribution rate evaluation based on operational network reliability. Systems Engineering and Electronics, 2021, 43(7): 1875–1883. (in Chinese)

[6] CHEN L, KOU Y X, LI Z, et al. Empirical research on complex networks modeling of combat SoS based on data from real war-game, Part I: statistical characteristics. Physica A: Statistical Mechanics and its Applications, 2018, 490: 754–773.

[7] SHI L K, PEI Y, YUN Q J, et al. Agent-based effectiveness evaluation method and impact analysis of airborne laser weapon system in cooperation combat. Chinese Journal of Aeronautics, 2023, 36(4): 442–454.

[8] GAO Y, LIU H, ZHOU Y M. An evaluation method of combat aircraft contribution effectiveness based on mission success space design. International Journal of Aeronautical and Space Sciences, 2019, 20: 273–286.

[9] XIE X Y, WEN S H, LI M L, et al. Resilience evaluation and optimization for an air-ground cooperative network. Electronic Research Archive, 2024, 32(5): 3316–3333.

[10] CHEN K B, LU Y J, GUO L, et al. A genetic algorithm-based methodology for analyzing the characteristics of high-operational-capability combat networks. IEEE Access, 2022, 10: 14717–14730.

[11] WANG Y, TAO J Y, ZHANG X K, et al. Mission-oriented capability evaluation for combat network based on operation loops. Defence Technology, 2024, 42: 156–175.

[12] GAO Y, CHENG J Y, TIAN Y L, et al. Machine learning-based evaluation of the contribution effectiveness in SoS missions. IEEE Systems Journal, 2023, 17(4): 5877–5888.

[13] ZHANG J G, FANG Z G, DONG W J. A novel equipment contribution evaluation framework for ESoS from a comprehensive perspective. Expert Systems with Applications, 2025, 265: 126042.

[14] WEN X X, TU C L, WU M G. Node importance evaluation in aviation network based on “No Return” node deletion method. Physica A: Statistical Mechanics and its Applications, 2018, 503: 546–559.

[15] XU T X, CHEN Y Q, LU C, et al. Importance measure of equipment task based on operational dependency of SoS. IEEE Access, 2021, 9: 15452–15466.

[16] TAN Y J, ZHANG X K, YANG K W. Research on networked description and modeling methods of armament system-of-systems. Journal of Systems & Management, 2012, 21(6): 781–786.

[17] PAN X, WANG H X, YANG Y J, et al. Resilience based importance measure analysis for SoS. Journal of Systems Engineering and Electronics, 2019, 30(5): 920–930.

[18] YANG K W, XIA B Y, CHEN G, et al. Multi-objective optimization of operation loop recommendation for kill web. Journal of Systems Engineering and Electronics, 2022, 33(4): 969–985.

[19] LUO C K, CHEN Y X, WANG L L, et al. Effectiveness

evaluation method of system-of-systems based on operation loop and improved information entropy. Systems Engineering and Electronics, 2019, 41(1): 73–80. (in Chinese)
[20] SHAO R R, FANG Z G, GAO S, et al. PS-G-GERT effectiveness evaluation model of link-based GEO satellite communication constellation under poor information background. China Communications, 2022, 19(12): 176–196.
[21] WANG Z, LIU S F, FANG Z G. Research on SoS-GERT network model for equipment system of systems contribution evaluation based on joint operation. IEEE Systems Journal, 2020, 14(3): 4188–4196.
[22] PENG L, LI J C, XIA B Y, et al. Weapons equipment portfolios selection based on equipment system contribution rates. Journal of Systems Engineering and Electronics, 2021, 32(3): 584–595.
[23] FAIGLE U, KERN W. The Shapley value for cooperative games under precedence constraints. International Journal of Game Theory, 1992, 21(3): 249–266.
[24] AN Q X, WEN Y, DING T, et al. Resource sharing and payoff allocation in a three-phase system: integrating network DEA with the Shapley value method. Omega, 2019, 85: 16–25.
[25] FANG F, YU S Y, LIU M X. An improved Shapley value-based profit allocation method for CHP-VPP. Energy, 2020, 213: 118805.
[26] ZHAO Y L, HAN F W, ZENG J F, et al. Coordinated optimization of integrated rural multiple regional energy systems considering electricity to ammonia and improved Shapley value revenue allocation. Energy, 2024, 313: 133855.
[27] SHARMA S, ABHYANKAR A R. Loss allocation for weakly meshed distribution system using analytical formulation of Shapley value. IEEE Trans. on Power Systems, 2016, 32(2): 1369–1377.
[28] LIU X X, WANG X S, GUO H Y, et al. Benefit allocation in shared water-saving management contract projects based on modified expected shapley value. Water Resour Managze, 2021, 35(1): 39–62.
[29] LOUHICHI M, NESMAOUI R, MBAREK M, et al. Shapley values for explaining the black box nature of machine learning model clustering. Procedia Computer Science, 2023, 220: 806–811.
[30] CHU C C F, CHAN D P K. Feature selection using approximated high-order interaction components of the Shapley value for boosted tree classifier. IEEE Access, 2020, 8: 112742–112750.
[31] ERRAZURIZ C, GOMEZ-LOBO A. A new look at the distributive incidence of Chile's means-tested water subsidy scheme. Water Policy, 2024, 26(7): 685–706.
[32] TAO Y L, WANG L, QI X X, et al. Grey Shapley value model for evaluating the contribution rate of weapon and equipment systems. Chinese Journal of Management Science, 2024, 32(4): 89–96. (in Chinese)
[33] LI S W, CHU L, WANG J S, et al. A road data assets revenue allocation model based on a modified Shapley value approach considering contribution evaluation. Scientific Reports, 2024, 14(1): 5179.
[34] LE P H, NGUYEN T D, BEKTAS T. Efficient computation of the Shapley value for large-scale linear production games. Annals of Operations Research, 2020, 287(2): 761–781.
[35] WANG L, LI Y H, WANG Y Q, et al. Compensation benefits allocation and stability evaluation of cascade hydropower stations based on variation coefficient-Shapley value method. Journal of Hydrology, 2021, 599: 126277.
[36] WU W L, ZHOU X S, SHEN B. Comprehensive evaluation of the intelligence levels for unmanned swarms based on the collective OODA loop and group extension cloud model. Connection Science, 2022, 34(1): 630–651.
[37] LI J C, GE B F, ZHAO D L, et al. Meta-path-based weapon-target recommendation in heterogeneous combat network. IEEE Systems Journal, 2019, 13(4): 4433–4441.
[38] LI J C, ZHAO D L, GE B F, et al. Disintegration of operational capability of heterogeneous combat networks under incomplete information. IEEE Trans. on Systems, Man, and Cybernetics: Systems, 2020, 50(12): 5172–5179.
[39] LIANG J L, XIONG W. Capabilities assessment of the weaponry system based on combat ring. Journal of Systems Engineering and Electronics, 2019, 41(8): 1810–1819.(in Chinese)
[40] ZHAO D L. Research on contribution rate of weapon and equipment system evaluation method based on heterogeneous network. Changsha: National University of Defense Technology, 2019. (in Chinese)
[41] YANG J B, XU D L. Evidential reasoning rule for evidence combination. Artificial Intelligence, 2013, 205: 1–29.
[42] ZHANG P, ZHOU Z J, TANG S W, et al. On the evidential reasoning rule for dependent evidence combination. Chinese Journal of Aeronautics, 2023, 36(5): 306–327.
[43] ZHAO F J, ZHOU Z J, HU C H, el al. A new evidential reasoning-based method for online safety assessment of complex systems. IEEE Trans. on Systems, Man, and Cybernetics: Systems, 2018, 48(6): 954–966.
[44] CHEN W Y, LI W M, ZHANG T, et al. Calculation of system combat capability using an interactive network approach. Acta Armamentarii, 2023, 44(10): 2885–2896.(in Chinese)
[45] GAO J W, YANG X F, LIU D. Uncertain Shapley value of coalitional game with application to supply chain alliance. Applied Soft Computing, 2017, 56: 551–556.